HAL
open science

Configurational mechanics in granular media

François Nicot, Mingchun Lin, A. Wautier, Richard Wan, F. Darve

To cite this version:

François Nicot, Mingchun Lin, A. Wautier, Richard Wan, F. Darve. Configurational mechanics in granular media. Granular Matter, 2024, 26 (3), pp.74. 10.1007/s10035-024-01443-1 . hal-04793912

HAL Id: hal-04793912

https://hal.inrae.fr/hal-04793912v1

Submitted on 17 Dec 2024

HAL is a multi-disciplinary open access archive for the deposit and dissemination of scientific research documents, whether they are published or not. The documents may come from teaching and research institutions in France or abroad, or from public or private research centers.

L'archive ouverte pluridisciplinaire **HAL**, est destinée au dépôt et à la diffusion de documents scientifiques de niveau recherche, publiés ou non, émanant des établissements d'enseignement et de recherche français ou étrangers, des laboratoires publics ou privés.

Copyright

Configurational mechanics in granular media

Francois Nicot[1], Mingchun Lin[1,5], Antoine Wautier[2], Richard Wan[3], and Félix Darve[4]

(1) Université Savoie Mont Blanc, ISTerre, Chambéry (France)
(2) Aix-Marseille Université, INRAE, Unité de Recherche RECOVER, Aix-en-Provence (France)
(3) University of Calgary, Calgary (Canada)
(4) Université Grenoble-Alpes, Laboratoire L3SR, Grenoble (France)
(5) Wuhan University, Wuhan (China)
Corresponding author: francois.nicot@univ-smb.fr

ABSTRACT:

Granular materials belong to the class of complex materials within which rich properties can emerge on large scales despite a simple physics operating on the microscopic scale. Most notable is the dissipative behaviour of such materials mainly through non-linear frictional interactions between the grains which go out of equilibrium. A whole variety of intriguing features thus emerges in the form of bifurcation modes in either patterning or un-jamming. This complexity of granular materials is mainly due to the geometrical disorder that exists in the granular structure. Diverse configurations of grain collections confer to the assembly the capacity to deform and adapt itself against different loading conditions. Whereas the incidence of frictional properties in the macroscopic plastic behavior has been well described for long, the role of topological reorganizations that occur remains much more elusive. This paper attempts to shed a new light on this issue by developing ideas following the configurational entropy concept within a proper statistical framework. As such, it is shown that contact opening and closing mechanisms can give rise to a so-called configurational dissipation which can explain the irreversible topological evolutions that granular materials undergo in the absence of frictional interactions.

KEYWORDS:

Granular materials, Continuum thermodynamics, Statistical mechanics, Loop transformation, Configurational transformation, Configurational entropy, Configurational granular mechanics, Boltzmann entropy, Shear band, Critical state regime, Bifurcation.

1. INTRODUCTION

Granular materials stand as the archetype of materials that offer a variety of remarkable features, despite an *a priori* very simplistic composition of individual particles interacting collectively at contacts. The mechanical properties of granular assemblies have attracted much interest within many scientific communities, ranging from soil mechanics to statistical physics (Duran, 2000; De Gennes *et al*., 2002; Parisi *et al*., 2017). As an illustration, it has been shown that, when loaded along a given mechanical loading path, granular materials can enter bifurcation regimes where the occurrence of various alternate failure modes is possible (Wan *et al*., 2017). In fact, despite granular materials displaying seemingly elementary particle configurations at the mesoscopic level, they yet represent an ideal example of complex systems where the existence of several, separate scales—from the grain scale to the specimen scale through the mesoscale—gives rise to emergent, salient properties at the upper scale. On another note, the behavior of granular materials is also closely related to the second law of thermodynamics that refers to the notion of entropy with the irreversibility of processes necessitating a positive change in entropy. A thermodynamic process will always evolve so long the maximum amount of work that can be extracted from it is minimized.

To understand thermodynamics, the concept of microstates versus macrostates has been developed within a statistical framework by Boltzmann in the second part of the nineteen's century and extended later by Gibbs through the notion of statistical canonical ensembles. We can normally measure the state variables characterizing a microstate, such as pressure as an intensive variable, whereas the microstates consisting of kinetic information (position and velocity) about all the individual molecules or atoms constituting the system are inaccessible except from a statistical viewpoint. This was the basic argument favoring the illuminating statistical approach initiated by Maxwell and Boltzmann (Maxwell, 1860; Boltzmann, 1877), then extended and formalized in a convenient statistical physics framework by Gibbs (1902).

From a statistical viewpoint, a system will always tend to adopt a macrostate that corresponds to the largest number of microstates, which means that the number of microstates is maximized. This fundamental idea is embedded within the famous H-theorem demonstrated by Boltzmann in 1872, giving way to the statistical interpretation of the second law of thermodynamics, reformulated later on through the celebrated Boltzmann's formula $S = k \ln \Omega$ that relates entropy S to the number Ω of microstates compatible with the

macroscopic state. In short, the probability of achieving a macrostate is proportional to the number of possible compatible microstates. Referring to the microcanonical ensemble statistics for isolated systems, the probability of all compatible microstates is the same. In other words, as stated in the ergodicity postulate, an isolated system at equilibrium will occupy successively all the accessible microstates for the same duration, assuming that a sufficiently large time range is considered.

Recently, this general framework of statistical physics has attracted some attention in granular solid mechanics as the system is constituted by a set of individual granules that can interact with each other. At a first glance, it could be tempting to apply the above framework to these materials by just regarding the granules as the molecules in a liquid or a gas. This pioneering idea dates to three decades ago and can be attributed to Edwards' paper (Edwards and Oakeshott, 1989) where the typical case of powders was considered. As powder particles are very fine, any macroscopic specimen contains a huge number of constituents so that the classical concepts of statistical physics can be applied within a certain degree of confidence.

In the Edward's paper, it is shown that unlike gas or liquids, the volume could play the role of kinetic energy, then proposing the measure of compactness as a convenient notion equivalent to the thermodynamic temperature. This was the first attempt paving the road to many contributions situated along this line of reasoning (see for example Baule *et al*, 2018; Jaeger *et al*. 1996; Kadanoff, 1999; Blumenfeld and Edwards, 2003 and 2014). In particular, granular gas and fluids (very loose granular matter) were systematically described by applying concepts borrowed from statistical mechanics as these materials are first and foremost disordered ones whose internal variables such as particle locations or velocities are random fields that can be described through a suitable statistics (Liu and Nagel, 1998; Silbert, 2005). One key concept was the introduction of granular temperature, constructed in a similar way as in statistical physics from the root mean square of the difference between the mean velocity and the actual particle velocity field; see for example, a detailed review of this question in Goldhirsch, 2008; Serero *et al*., 2008).

When it comes to investigating the case of granular solids which are dense granular matter, several issues arise. In particular, the high compactness of these materials compromises a direct application of the above-mentioned particle velocity concepts. It turns out that the governing mechanisms within granular solids are totally different from those taking place

within granular fluids and gas, mainly governed by the velocity field of particles that collide and move along a free path between successive collisions. By contrast, processes that occur on the microscopic scale within a granular solid are mainly dictated by the mechanical interaction of particles at contacts. All contacts flock together to form a fabric pattern made up of small grain clusters involving a few grains. These clusters degenerate into so-called grain loops in 2D conditions (Tordesillas *et al*., 2012; Pucilowski *et al*., 2020; Walker *et al*., 2015). In addition, nearly linear chains, called force chains and carrying the main fraction of the internal contact forces, develop within the assembly (Radjai *et al*., 1998; Peters *et al*., 2005). In line with Edwards' conjecture, it is thus believed that such materials can be couched within the above thermodynamic framework.

Restricting henceforth our analysis to two-dimensional specimens and exploring further an illuminating idea suggested by Wanjura *et al*. (2020) and Sun *et al*. (2020), the number of microstates in the assembly can be likened to the myriad of mesoscopic loops the collection of particles can form so that their evolution (genesis and breakage) is reminiscent of a chemical reaction. Also, the propensity or spontaneity of a change in loops topology is just like what happens in the kinetics of a chemical reaction dictated by entropy and rate of reactions, here again within the frame of the second law of thermodynamics.

The manuscript will be organized as follows. The basic thermochemistry background will be first reviewed in section 2, and the constitutive concepts of a proper configurational granular mechanics will be developed in section 3, leading to the introduction of a configurational entropy term. Then, section 4 will elaborate an extension of the continuum thermodynamic framework to include the concepts of the configurational granular mechanics. Finally, a closing discussion will shed light on the potential advances that can be realized in the framework of such a proposed approach.

2. THERMOCHEMISTRY BACKGROUND

We consider in this section a mixture of m different chemical species C_i that can react with each other so that the number N_i of each compound of a given species 'i' can evolve. Classically, a chemical reaction involves reactive compounds that can react with each other to

form products. Adopting a general formalism, the chemical transformation operating within the mixture can be expressed as:

$$\nu_1 C_1 + \nu_2 C_2 + \cdots + \nu_m C_m = 0 \tag{1}$$

where ν_i is the stochiometric coefficient of the species 'i' with ν_i being positive for products, and negative for reactive species.

The effect of a change in the number of compounds N_i on the internal energy U of the system is described by Gibbs' equation which involves the chemical potential $\mu_i = \left(\frac{\partial U}{\partial N_i}\right)_{S,V,N_j}$ of each species as follows:

$$\dot{U} = \theta \dot{S} - P \dot{V} + \sum_{i=1}^{m} \mu_i \dot{N}_i \tag{2}$$

where S is the entropy of the system at a given thermodynamic temperature θ and pressure P. Eq. (2) can be thus rearranged as:

$$\dot{S} = \frac{1}{\theta} \dot{U} + \frac{P}{\theta} \dot{V} - \sum_{i=1}^{m} \frac{\mu_i}{\theta} \dot{N}_i \tag{3}$$

where the chemical potential of the species 'i' now reads:

$$\mu_i = -\theta \left(\frac{\partial S}{\partial N_i}\right)_{U,V,N_j} \tag{4}$$

The chemical reaction of species, as expressed in Eq. (4), undergoes the concept of chemical affinity A, defined as:

$$A = -\sum_{i=1}^{m} \nu_i \mu_i \tag{5}$$

By invoking the notion of extent of reaction ξ, with $\dot{N}_i = \nu_i \dot{\xi}$, the internal entropy production due to the extension of the chemical reaction under constant internal energy and volume reads:

$$\dot{S} = \frac{A \dot{\xi}}{T} = -\sum_{i=1}^{m} \frac{\mu_i}{T} \dot{N}_i \tag{6}$$

Equation (6) allows the entropy production to be expressed in a standard formalism as the product of a thermodynamic force (chemical affinity divided by the thermodynamic temperature) and a conjugate flux (rate of extent of reaction). The second law of thermodynamics imposes that $A\dot{\xi} \geq 0$. In other words, the system will evolve (i.e., the chemical reactions extent) until the affinity vanishes: $A = 0$. It is worth mentioning that once the affinity is zero, the system is in a stationary state where chemical reactions may continue progressing in a way that the fraction $\alpha_i = \frac{N_i}{N}$ of each species remains constant on average, with $N = \sum_i^m N_i$ being the total number of compounds.

It is useful at this stage to draw the parallel with the topology change of loops of different orders (i.e., number of particles) that occur within a granular system (Wanjura *et al*., 2020; Sun *et al*., 2020). The topological evolution of loops can be compared to some extent with a chemical reaction in the sense that chemical reactions are governed by chemical bonding processes involving the sharing or loss of electrons in the outermost layer, while granular materials under an external mechanical loading experience a contact activity by forming or losing contacts between adjoining grains, which leads to new loop topologies.

In order to exploit the above-mentioned analogy, it is convenient to describe a two-dimensional granular assembly as a set of elementary, interconnected grain loops (Fig. 1). Grain loops are minimally closed contact chain structures with the number of grains involved in a given loop defining the loop order. Thus, a loop containing *i* grains will be denoted L_i. Referring to the fundamentals of statistical physics, a granular assembly in a given mechanical state (macroscopic state) defined by a set of macroscopic variables (such as the stress field), can therefore be associated with a set of microscopic states characterized by the topological configuration of the grains through a distribution of loops. By analogy with statistical physics, all the loop distributions compatible with the macroscopic state thus constitute a statistic ensemble denoted as a canonical ensemble.

The key idea of this manuscript is to borrow the concepts of thermochemistry recalled herein to describe the evolution of the topological microstructure within a granular assembly. This is

done by drawing a link between the notion of chemical reaction of species and the notion of ‘topological’ reaction within a collection of elementary loops that can reorganize themselves by gaining or losing a contact.

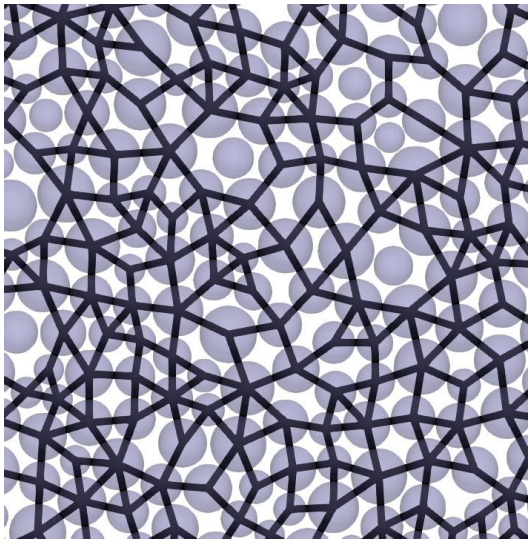

Fig. 1. Example of a loop tessellation in a 2D granular assembly. The tessellation is obtained by joining the centers of the particles in contact with branch lines, forming polygons. Each polygon corresponds to a specific loop, the number of sides giving the order of the loop (after Liu *et al*., 2020)

3. THE CONCEPT OF CONFIGURATIONAL GRANULAR MECHANICS

3.1 Preamble

We consider a system consisting of a given two-dimensional granular material, initially in a configuration C_o (initial configuration) with a volume V_o (with $\Gamma_o = \partial V_o$). After a loading history, the system is in a strained configuration C and occupies a volume V (with $\Gamma = \partial V$), and is supposed to be in mechanical equilibrium under the current prescribed external loading. This loading is imposed through either boundary static or kinematic parameters, referred to as the control parameters, that make the entropy evolve while energy exchanges develop. The entropy production $\dot{S}$ (rate of entropy) of the system can be split into the internal entropy production $\dot{S}^{\text{int}}$ (involving the entropy produced within the system) and the external entropy production $\dot{S}^{ext}$ (concerning the entropy exchanged through the boundary of the system with the external world), i.e.

$$\dot{S} = \dot{S}^{\text{int}} + \dot{S}^{ext} \tag{6}$$

In soft matter physics, granular materials under standard mechanical loading are considered athermal, glassy materials (Parisi, 2012; Bi *et al*., 2015) where thermal fluxes can be omitted as a first approximation. The thermodynamic temperature is assumed constant. This assumption is reasonable in most situations but can fail when dealing with very large-scale problems such as in earthquakes where the mobilized frictional energy under very high tectonic pressures induces fast and significant temperature rises. As shown in Nicot *et al*. (2023), the internal entropy production $\dot{S}^{\text{int}}$ is proportional to the plastic dissipation power $\dot{W}^{pl} = \int_V \sigma_{ij}\, \dot{\varepsilon}_{ij}^{p}\, dv$:

$$\dot{S}^{\text{int}} = \frac{1}{\theta} \int_V \sigma_{ij}\, \dot{\varepsilon}_{ij}^{p}\, dv \tag{7}$$

where θ is the thermodynamic temperature of the system, and $\boldsymbol{\sigma}$ (resp. $\dot{\boldsymbol{\varepsilon}}^{pl}$) corresponds to the Cauchy stress tensor (resp. the plastic part of the strain tensor rate) field acting within the system. Basically, plastic dissipation within athermal granular systems stems from the frictional sliding or rotations at contacts between adjoining particles (Nicot and Darve, 2007). It is well admitted that the frictional dissipation between two solids in contact along an interface plane can be described by Coulomb's law, which states that sliding occurs whenever

the tangential contact force F_t within the tangent plane equals the normal contact force F_n multiplied by the friction coefficient μ. The Coulomb criterion reads therefore:

$F_t < \mu F_n$ no sliding occurs (8a)

$F_t = \mu F_n$ the sliding can occur along the interface (8b)

Thus, the system reorganizes itself through microstructural rearrangements stemming from the relative motion between the grains. An often-debated question then arises: What happens when the friction between the particles is ideally set to zero? In such a case, Eq. (8b) imposes that sliding occurs in any contact plane under zero tangential force. It turns out that the specimen mainly rearranges in an irreversible way under external loading with no frictional dissipation. Whereas the microstructure evolves irreversibility, Eq. (7), as such, leads to the counter-intuitive result that no entropy production takes place. This comes to infer that Eq. (7) might be incomplete, suggesting the existence of a missing term capable of properly accounting for microstructural evolutions alone, irrespective of any frictional dissipation contribution. It is thought that this missing term can be identified with the so-called configurational entropy.

The concept of configurational entropy introduced in the middle of the last Century (Gibbs and Dimarzio, 1958; Adam and Gibbs, 1965) was repeatedly proposed as a way to express the entropy of discrete, athermal media by taking inspiration from Boltzmann's approach (Preisler and Dijkstra, 2016), or, equivalently, from Shannon's information theorem (Shannon, 1948). It should be noted that both theories have been demonstrated to be equivalent by Jaynes, in 1957; see, for example, a complete overview in (Jaynes, 1957 and 1983).

The range of eligible materials encompassing configurational entropy goes far beyond granular materials, including for example biology components such as proteins (Doig and Sternberg, 1995). Basic approaches were essentially developed by advocating the existence of a probability density function modeling the randomness of a given topological descriptor such as the contact distribution in granular-like assemblies.

In this work, we propose an alternative approach, rooted in a different understanding of granular media. Basically, a granular solid is governed by both grain sliding and contact

opening or closing. These two mechanisms can be regarded as the core ingredients that control the mechanical response of a granular assembly under a given loading. Grain sliding causes deformation of loops, and therefore (frictional) plastic dissipation related to a large fabric rearrangement. On the other hand, contact losses and gains cause a configurational change with no frictional dissipation. Both of them are obviously linked as particles sliding, when large enough, can induce contact opening or closing, which in turn leads to microstructural rearrangements. Thus, a way to account for these physical ingredients is to introduce an additional entropy term that specifically accounts for the contact opening or closing, without any plastic effect.

The contact opening and closing mechanism is associated with the concept of configurational entropy that will be detailed out in the next section, while frictional plasticity processes are associated with the classical internal entropy as given in Eq. (6). We shall emphasize that the configurational entropy developed in this work refers to an instantaneous event, consisting of contact creation or deletion, excluding any finite grain motion. By the same token, the entropy variation related to a chemical reaction refers to the creation or deletion of chemical bonds, in exclusion of any diffusion effect involving atomic or molecular motion within the chemical mixture.

The purpose of the next sections is to derive the expression of this configurational entropy by elaborating a novel framework herein denoted as the configurational granular mechanics.

3.2 Configurational framework for an elementary granular reaction

The granular system introduced in section 3.1 can be described, from a microstructural point of view, by a microstate E^{mic} corresponding to a distribution of loops L_i . It is convenient to express E^{mic} as follows:

$$E^{\mathrm{mic}} = \left\{ \left(L_3, N_3 \right), \left(L_4, N_4 \right), \ldots, \left(L_m, N_m \right) \right\} \tag{9}$$

where the collection set includes all the loops and orders contained in the assembly at a given state.

The order of loops ranges from a minimal size (equal to 3) to a maximal size m (Tordesillas *et al*., 2012; Walker *et al*., 2015; Zhu *et al*., 2016a and 2016b; Pucilowski and Tordesillas, 2020; Deng *et al*., 2022). For a given macrostate E^{mac} controlled by the boundary conditions and described from extensive variables such as the stress state, a very large number n_E of related microstates E^{mic} exists, corresponding to all loop distributions compatible with E^{mac}.

As previously mentioned, all these compatible microstates constitute a canonical ensemble. Basically, the order of magnitude of n_E scales with N^m, where N is the number of particles contained in the assembly. Under an incremental change in the boundary conditions, the loop distribution will evolve from a given microstate E_1^{mic} to a new microstate E_2^{mic}. Inspired by the pioneering ideas presented in Wanjura *et al*. (2020) to build a rational framework for describing the detailed balance of topological changes in a 2D granular assembly, we consider that the loop distribution evolves through elementary, instantaneous loop transformations referred to as elementary configurational reactions. Ignoring as a first approximation the generation of rattlers, these configurational reactions, as exemplified in Fig. 2, can be formulated as follows in a very general way:

$$(R_{i,j}) \quad L_i \rightleftarrows L_j + L_{i+2-j} \tag{10}$$

for any $i \in \{4, \ldots, m\}$, with $j < i$

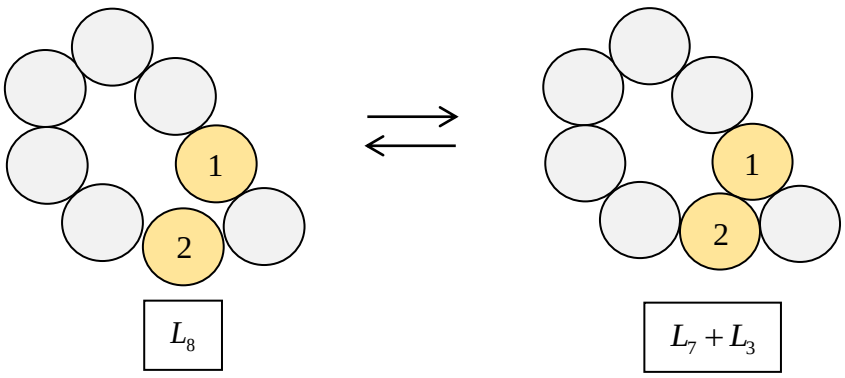

Fig. 2. Example of an elementary configurational reaction. A loop with 8 grains transforms reversibly into a loop with 7 grains and a loop with 3 grains by contact opening/closing between grains 1 and 2.

Turning to the mesoscopic scale, the configurational reaction $R_{i,j}$ transforms reversibly the meso-configuration $C(i, 0)$ into the meso-configuration $C(j, i+2-j)$, where the arguments

between brackets correspond to the order of loops composing each of the two meso-configurations. Over an infinitesimal duration dt, let $dN_{i,j}$ be the infinitesimal change in the amount of loops L_i through the configurational reaction $R_{i,j}$ taking place within the assembly. We do recall that all reactions are considered instantaneous. Thus, the extent of the configurational reaction, by analogy with the thermochemistry formalism, is given by $d\xi_{i,j} = -dN_{i,j}$. As both reactions $R_{i,j}$ and $R_{i,i+2-j}$ are identical, it is worth noting that $dN_{i,j} = dN_{i,i+2-j}$.

It is emphasized here that the configurational approach proposed in this manuscript focuses on the contact network, and its evolution over contact gain and loss that entail closed loops evolution. This key idea constitutes the basis of the subsequent configurational granular mechanics.

Let's consider an isolated loop L_i containing i distinguishable particles and i contacts. If the chain of particles was not closed, there would be $i!$ different possible configurations to arrange the i contacts. A configuration consists of a sequence of the i contacts (and therefore of the i grains), irrespective of the geometrical shape of the chains. For a closed loop, there will be $(i-1)!$ different configurations, as all the i cyclic permutations should be removed.

By denoting $S_{i,0}$ the entropy of the configuration $C(i,0)$, composed of a unique loop of order *i*, and postulating a connection with Boltzmann's formula, the entropy can be ideally expressed as a function of the number of compatible microstates, i.e.,

$$S_{i,0} = k \ln(i-1)! \tag{11}$$

where *k* is a Boltzmann-like constant, the magnitude of which should depend on the effective number of grains under consideration and a large enough number of configurations of grain arrangements to define an ensemble average as the state of the system.

It should be recalled that for large systems such as usual (molecular) gases and liquids, the number of particles (atoms or molecules) is typically on the order of the Avogadro's number,

i.e. 10^{23} , which scales with the inverse of the standard Boltzmann constant, $k_B \approx 1.38\,10^{-23}$ J.K^{-1}.

In a similar way, the configuration $C\left(j, i+2-j\right)$ is composed of two loops L_j and L_{i+2-j}, that will be assumed to be isolated from any external constraints. Each of the two loops constitutes a set of contacts (j contacts and $i+2-j$ contacts) that will be all considered distinct from each other. As such, the entropy $S_{j,i+2-j}$ of the configuration $C\left(j, i+2-j\right)$ can therefore be expressed as:

$$S_{j,i+2-j} = k\,\ln\left(j-1\right)! + k\,\ln\left(i+1-j\right)! = k\,\ln\left(\left(j-1\right)!\left(i+1-j\right)!\right) \tag{12}$$

By analogy with the chemical potential defined in Eq. (4), we introduce the notion of configurational potential μ_i associated with the loop L_i, as follows:

$$\mu_i = k\,\theta\,\ln\left(i-1\right)! \tag{13}$$

The physical meaning of this potential is that the more contacts a loop has, the higher its propensity to split into 2 smaller loops.

Again, by analogy with the chemical affinity previously defined in Eq. (5), the notion of configurational affinity $A_{i,j}$ associated with the reaction $R_{i,j}$, can readily be defined as:

$$A_{i,j} = -\left(-\mu_i + \mu_j + \mu_{i+2-j}\right) = k\,\theta \ln\left(\frac{(i-1)!}{(j-1)!\,(i+1-j)!}\right) \tag{14}$$

Straightforward algebraic manipulations make it possible to show that $A_{i,j}$ is a strictly positive quantity (see Appendix A1). Thus, the configurational entropy production $\dot{S}_{i,j}^{conf}$ related to the reactions $R_{i,j}$ can be written as:

$$\dot{S}_{i,j}^{conf} = \frac{A_{i,j}}{\theta}\,\dot{\xi}_{i,j} = \frac{\mu_i - \mu_j - \mu_{i+2-j}}{\theta}\,\dot{\xi}_{i,j} \tag{15}$$

that is:

$$\dot{S}_{i,j}^{conf} = -k \ln\left(\frac{(i-1)!}{(j-1)!\,(i+1-j)!}\right)\dot{N}_{i,j} \tag{16}$$

From Eq. (15), it can be inferred that whenever the reaction $R_{i,j}$ advances toward the right-hand side ($\dot{\xi}_{i,j} > 0$), forming two smaller loops L_j and L_{i+2-j}, the configurational entropy production $\dot{S}_{i,j}^{conf}$ is strictly positive. It is negative along the reverse way, when a larger loop L_i is formed from two smaller ones. The direction of the configurational reaction is therefore governed by the potentials of the different loops under consideration. If the potential of L_j (left hand loop) is greater than the potential of $L_j + L_{i+2-j}$ (right hand loops), the reaction progresses toward the right, that is from the highest potential toward the lowest potential. This clarifies the meaning of the configurational affinity, that characterizes the propensity of the reaction to progress toward a particular side.

3.3 Ensemble of configurational granular reactions

A rational framework has been developed in the previous section to describe a single, elementary reaction $R_{i,j}$. Over an infinitesimal duration dt, a distribution of $dN_{i,j}$ reactions $R_{i,j}$ take place within the whole granular assembly, with $3 \le j \le \text{int}(i/2)+1$ and $4 \le i \le m$. The distribution is limited to $j \le \text{int}(i/2)+1$, as reactions $R_{i,j}$ and $R_{i,i+2-j}$ are identical. According to the additivity property of the entropy, the configurational entropy production for the whole assembly can be expressed as:

$$\dot{S}^{conf} = \sum_{i=4}^{m} \sum_{j=3}^{\text{int}(i/2)+1} \dot{S}_{i,j}^{conf} = -\frac{\sum_{i=4}^{m} \sum_{j=3}^{\text{int}(i/2)+1} A_{i,j}}{\theta} \dot{N}_{i,j} \tag{17}$$

with $A = \sum_{i=4}^{m} \sum_{j=3}^{\text{int}(i/2)+1} A_{i,j}$ being the mutual affinity between all the configurational species composing the whole assembly.

The infinitesimal change dN_i in the number of loops L_i over a duration dt can be related to the infinitesimal change $dN_{i,j}$ in the amount of loops L_i through the reactions $R_{i,j}$. Indeed, a

loop L_i can merge with a loop L_{j+2-i} to form a larger loop L_j (with $i+1 \le j \le m$), or split into two smaller loops L_j and L_{i+2-j} (with $3 \le j \le \text{int}(i/2)+1$). Thus, we have:

$$dN_3 = -\sum_{j=4}^{m} \left(1+\delta_{i,j-1}\right) dN_{j,3} \qquad \text{when } i=3 \tag{18a}$$

$$dN_i = \sum_{j=3}^{\text{int}(i/2)+1} dN_{i,j} - \sum_{j=i+1}^{m} \left(1+\delta_{i,j+2-i}\right) dN_{j,i} \qquad \text{when } 4 \le i \le m-1 \tag{18b}$$

$$dN_m = \sum_{j=3}^{\text{int}(m/2)+1} dN_{m,j} \qquad \text{when } i=m \tag{18c}$$

where $\delta_{k,l}$ is the Kronecker symbol, with $\delta_{k,l}=1$ if $k=l$, and $\delta_{k,l}=0$ otherwise. It should be noted that for the particular situation where $j=2i-2$, the loop L_j splits into two identical loops L_i. For example, a loop L_4 can split in two loops L_3 when two opposite grains contact.

The configurational entropy of the assembly, as given in Eq. (17), can be rewritten by virtue of Eqs. (18). The following expression can readily be obtained (see Appendix A2):

$$\dot{S}^{conf} = -\frac{1}{\theta}\sum_{i=3}^{m} \mu_i \, \dot{N}_i + \frac{1}{\theta}\,\dot{\chi} \tag{19}$$

with $\dot{\chi} = \sum_{i=4}^{m} \sum_{j=3}^{\text{int}(i/2)+1} \left(\mu_j + \mu_{i+2-j}\right) \dot{N}_{i,j} - \sum_{i=3}^{m-1} \sum_{j=i+1}^{m} \mu_i \left(1+\delta_{i,j+2-i}\right) \dot{N}_{j,i}$.

Using tensorial manipulations, it can be shown that this last term is always nil with the proof of this result given in Appendix A3. This allows us to formally recover the classical Gibbs equation which was given in Eqs. (3) and (6) for the entropy of a mixture of *m* chemical reacting species under constant volume and internal energy. Thus, analogously we have the configurational entropy as:

$$\dot{S}^{conf} = -\frac{1}{\theta}\sum_{i=3}^{m} \mu_i \, \dot{N}_i \tag{20}$$

At this point, it should be stressed that the instantaneous contact opening and closing event is associated with no volume nor energy changes. As such, ending up with a relation that is

formally identical to the Gibbs equation should be regarded as a strong proof of consistency of the approach developed in this work.

4. EXTENDING THE CONTINUUM THERMODYNAMICS FRAMEWORK

4.1 Fundamentals of thermodynamics

The fundamentals of the standard continuum thermodynamics are first reviewed in this section. The internal energy of any material system is given by the first law of thermodynamics, i.e.

$$\dot{U} = \dot{Q} + \int_V \sigma_{ij}\ \dot{\varepsilon}_{ij}\ dv \tag{21}$$

where the heat power $\dot{Q}$ reads as:

$$\dot{Q} = \int_V \rho\ \dot{r}\ dv - \int_{\partial V} \dot{q}_i\ n_i\ ds \tag{22}$$

The first integral corresponds to the radiated heat within the system body, and the second integral accounts for the boundary conduction heat transfer with a heat flux $\dot{\mathbf{q}}$.

Equation (21) expresses the internal energy U within the system in an integral form. Noting $U = \int_V \rho\ e\ dv$, where e denotes the specific internal energy and ρ the local density of the material, Eq. (21) can be expressed following a local formulation as:

$$\rho\ \dot{e} = \rho\ \dot{r} + \sigma_{ij}\ \dot{\varepsilon}_{ij} - \frac{\partial \dot{q}_i}{\partial x_i} \tag{23}$$

As we have $\dot{S} = \dot{S}^{ext} + \dot{S}^{\text{int}}$, with

$$\dot{S}^{ext} = \frac{\dot{Q}}{\theta} = \int_V \rho\ \frac{\dot{r}}{\theta}\ dv - \int_{\partial V} \frac{\dot{q}_i}{\theta}\ n_i\ ds \tag{24}$$

and

$$\dot{S}^{int} = \int_V \frac{\Phi}{\theta}\ dv \tag{25}$$

where Φ denotes the total dissipation rate within the system, and noting $S = \int_V \rho\ \eta\ dv$, where η is the specific entropy, it can be shown that:

$$\Phi = \rho\,\theta\,\dot{\eta} - \rho\,\dot{r} + \frac{\partial \dot{q}_i}{\partial x_i} - \frac{\dot{q}_i}{\theta}\frac{\partial \theta}{\partial x_i} \tag{26}$$

where the term $\Phi^{\text{int}} = \rho\,\theta\,\dot{\eta} - \rho\,\dot{r} + \frac{\partial \dot{q}_i}{\partial x_i}$ stands for the intrinsic dissipation rate, whereas the term $\Phi^{th} = -\frac{\dot{q}_i}{\theta}\frac{\partial \theta}{\partial x_i}$ represents the conduction heat dissipation rate. Eq. (26) leads to the classical Clausius-Duhem inequality.

4.2 Entropy as a combination of dissipative and configurational processes

We now introduce the effective specific entropy η^*, defined as the difference between the specific entropy η and the configurational part η^{conf}, with $S^{conf} = \int_V \rho\,\eta^{conf}\,dv$. Thus:

$$\eta^* = \eta - \eta^{conf} \tag{27}$$

It should be emphasized that the configurational entropy accounts only for the topological changes induced by instantaneous contact opening and closing events in the absence of any other processes such as grain sliding and rotation, or grain deformation. Therefore. the effective entropy corresponds to the usual entropy stemming from standard dissipation processes, excluding any configurational processes considered in this work. Thus, η^* can be related to the Helmholtz free energy through the classical Legendre transform:

$$\Psi = e - \theta\,\eta^* \tag{28}$$

Combining Eqs. (23) and (28) yields the following relation:

$$\rho\,\dot{\Psi} = \rho\,\dot{r} - \frac{\partial \dot{q}_i}{\partial x_i} - \Phi^{th} - \rho\,\dot{\theta}\,\eta^* - \rho\,\theta\left(\dot{\eta} - \dot{\eta}^{conf}\right) + \sigma_{ij}\,\dot{\varepsilon}_{ij} \tag{29}$$

which can be rearranged as:

$$\Phi^{\text{int}} + \Phi^{th} = -\rho\left(\dot{\Psi} + \dot{\theta}\,\eta^*\right) + \rho\,\theta\,\dot{\eta}^{conf} + \sigma_{ij}\,\dot{\varepsilon}_{ij} \tag{30}$$

Restricting the analysis to athermal materials makes it possible to omit the term $\dot{\theta}\,\eta^{*}$. Furthermore, the thermodynamic temperature within the material system is assumed to be constant (isothermal conditions), so that $\Phi^{th}=0$. Then, using the standard additive strain rate decomposition $\dot{\varepsilon}_{ij}=\dot{\varepsilon}_{ij}^{e}+\dot{\varepsilon}_{ij}^{p}$, with $\dot{\varepsilon}_{ij}^{e}$ being the elastic strain part and $\dot{\varepsilon}_{ij}^{e}$ being the plastic strain counterpart, yields:

$$\Phi^{\text{int}}=\sigma_{ij}\,\dot{\varepsilon}_{ij}^{e}-\rho\,\dot{\Psi}+\sigma_{ij}\,\dot{\varepsilon}_{ij}^{p}+\rho\,\theta\,\dot{\eta}^{conf} \tag{31}$$

Noting that the rate of the Helmholtz free energy is $\rho\,\dot{\Psi}=\sigma_{ij}\,\dot{\varepsilon}_{ij}^{e}$, the internal dissipation potential given in Eq. (31) reduces to:

$$\Phi^{\text{int}}=\sigma_{ij}\,\dot{\varepsilon}_{ij}^{p}+\rho\,\theta\,\dot{\eta}^{conf} \tag{32}$$

This corresponds to the intrinsic dissipation rate, which is always positive according to the second law of thermodynamics. It turns out that the intrinsic dissipation rate is composed of two terms. The first one, $\Phi^{\text{int},p}=\sigma_{ij}\,\dot{\varepsilon}_{ij}^{p}$, corresponds to the plastic (frictional-based) processes induced by grain sliding at contacts, while the second one, $\Phi^{\text{int},conf}=\rho\,\theta\,\dot{\eta}^{conf}$, pertains to the configurational transformation related to contacts opening and closing.

As $\dot{S}^{int}=\int_V \frac{\Phi^{\text{int}}}{\theta}\,dv=\int_V \rho\,\dot{\eta}^{\text{int}}\,dv$, where η^{int} corresponds to the specific internal entropy, it can also be written that:

$$\rho\,\dot{\eta}^{\text{int}}=\frac{1}{\theta}\sigma_{ij}\,\dot{\varepsilon}_{ij}^{p}+\rho\,\dot{\eta}^{conf} \tag{33}$$

Equation (33) constitutes a local formulation of the internal entropy production written at the material point scale. By extending the formulation to the whole granular assembly, it can eventually be obtained that:

$$\dot{S}^{\text{int}}=\int_V \frac{1}{\theta}\sigma_{ij}\,\dot{\varepsilon}_{ij}^{p}\,dv-\frac{1}{\theta}\sum_{i=3}^{m}\mu_i\,\dot{N}_i \tag{34}$$

where the configurational potential μ_i of each loop L_i is given by Eq. (13).

5. CLOSING DISCUSSION

5.1 Configurational irreversibility

Equation (34) embeds the important physical notion that the internal entropy, and thereby the dissipation potential, is composed of a plastic dissipation term due to sliding of particles and a complementary term stemming from transformations of the internal configurational topology. It should be emphasized that loops deform mainly through plastic sliding at contacts as well as rolling motion, inducing changes in the conformation of loops, i.e., their geometry and arrangement. If these changes do not give rise to contact opening and closing, the distribution of loops stays the same, and the dissipation within the system is entirely captured by the plastic term $\dot{S}^{\text{int},p} = \int_V \frac{1}{\theta} \sigma_{ij} \, \dot{\varepsilon}_{ij}^{p} \, dv$. Otherwise, when the deformation of the loops involves contact opening or closing, the mesostructures transform with potential subsequent changes in the loop distribution. The dissipation associated with this change in topology is properly described by the configurational term $\dot{S}^{\text{int},conf} = -\frac{1}{\theta} \sum_{i=3}^{m} \mu_i \, \dot{N}_i$ (for the sake of simplicity, and to stay consistent with the notations of section 3.2, this term will be noted $\dot{S}^{conf}$ in the sequel).

When it comes to deal with very low friction materials, such as lubricated assemblies, the contribution of the plastic dissipation in the entropy can become negligible. In the limiting and ideal case where the friction is ideally zero, the term $\dot{S}^{\text{int},p}$ disappears so that the entropy production is then solely supported by the configurational changes within the specimen. This is indeed meaningful as irreversible strains are expected to occur, whereas no plastic dissipation develops, and no plastic dissipation-based entropy production takes place.

It is crucial to quantify the direction of variation of $\dot{S}^{conf}$, according to the changes in configuration. As mentioned in section 3, the configurational entropy production $\dot{S}_{i,j}^{conf}$ is strictly positive whenever the reaction $R_{i,j}$ advances toward the right-hand side ($\dot{\xi}_{i,j} > 0$), forming smaller loops L_j and L_{i+2-j}, and is negative along the reverse way, when a larger loop L_i is formed. Thus, according to the second law of thermodynamics, it is expected that under a given loading, a frictionless granular specimen should evolve in a way that promotes

the creation of smaller loops. The largest loops disappear to the benefit of smaller ones, making the specimen contract and its specific volume decrease.

The above-mentioned result can indeed be checked from numerical simulations based on a discrete element method (Cundall and Strack, 1979). The mechanical response of a two-dimensional frictionless granular specimen, axially compressed under a constant lateral pressure, is simulated. As shown in Fig. 3, the configurational entropy, normalized by the Boltzmann-like constant, increases monotonously (from an initial, arbitrary zero value) until reaching an asymptotic value on average. The fluctuations observed in Fig. 3 will be discussed in section 5.3.

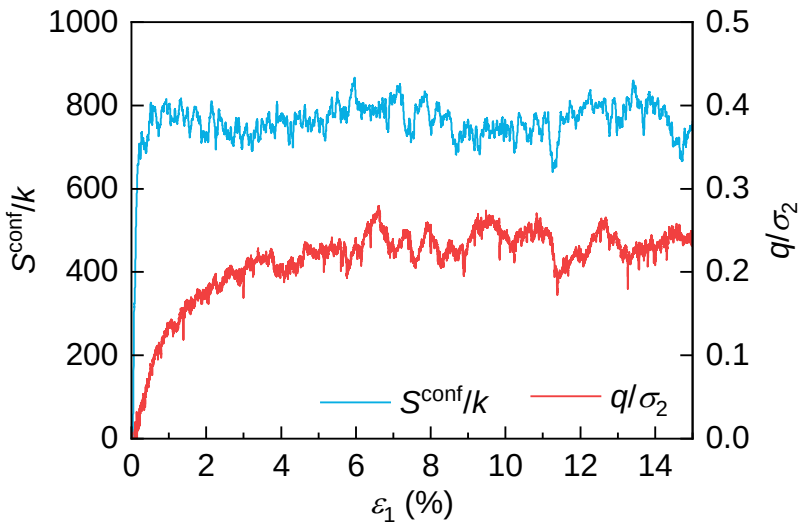

Fig. 3. Simulation of the response of a dense, frictionless 2D specimen made up of a polydisperse assembly of 20,000 spherical particles along a biaxial loading under a constant lateral stress of 100 kPa, by using a discrete element method (YADE open-source code, Smilauer *et al.*, 2015). The evolution of both the normalized deviatoric stress[1] and the configurational entropy is given in terms of the axial strain.

5.2 Critical state regime in the light of the configurational mechanics

As another illustration of the applicability of the configurational granular mechanics framework developed in this work, we propose to address and clarify in a general manner the issue of the critical state regime that occurs in solid materials under shearing. This intriguing feature has been questioning the scientific community for many decades (Roscoe *et al.*, 1958;

[1] The normalized deviatoric stress is given by q/σ_2, where $q=\sigma_1-\sigma_2$, σ_1 is the axial stress, and σ_2 is the constant lateral stress.

Been *et al*., 1991; Parisi *et al*., 2017; Liu *et al*., 2020; Deng *et al*., 2022). Granular materials experience an ultimate regime (denoted as the critical state regime), bringing the material to a unique mechanical state defined by a constant specific volume and a constant stress state, irrespective of the initial porosity of the material, while shear deformation processes are being maintained. Furthermore, for a sufficiently densely packed specimen, a phase transition is observed after a certain level of shearing coinciding with the formation of a strain localization pattern with one or multiple shear bands developing (Desrues and Andò, 2015). It was recently shown that this phase transition is consistent with the extremal entropy production theorems (Nicot *et al*., 2023), leading to an optimal dissipative structure (namely, the shear band pattern) able to dissipate the most part of the external energy put into the system, and making the system able to sustain external loading without collapsing (Wang *et al*., 2023).

It has repeatedly been observed that dense granular specimens under shearing experience a spontaneous break in symmetry transitioning to a lower state of energy before reaching the critical state regime. This break in symmetry corresponds to a phase transition from a statistically homogeneous state to a heterogenous one, giving way to a shear band pattern fully developed once the critical state regime is reached. Thus, the specimen is composed of different spatial domains, with totally different properties. While the domain located outside the shear band pattern remains dense with nearly no dissipation processes occurring, the domain inside the shear band undergoes a marked dilatancy associated with an intense plastic dissipation.

The above-described transition toward a structured material has recently been investigated (Nicot *et al*., 2023) by invoking the extremal entropy production theorems (Glansdorff and Prigogine, 1954, 1963 and 1964; Prigogine and Lefever, 1968; Veveakis and Regenauer-Lieb, 2015; Dewar, 2005; Ziegler, 1983; Janečka and Pavelka, 2018; Benfenati, and Beretta, 2018; Porporato *et al*., 2020; Lucarini *et al*., 2020). Such phase transitions can be encountered in various situations such as the Rayleigh-Bénard cells (Bénard, 1901; Rayleigh, 1916), the chemical clocks (Hudson and Mankin, 1981), or many biological processes based on cellular self-organizations. All these transitions might suggest that the second principle of thermodynamics is violated, as they give rise to a gain in order. In particular, the formation of the shear band is accompanied by a dilatant behavior promoting the formation of larger loops to the detriment of smaller ones. Thus, the configurational reactions given in Eq. (10) advance toward the left side, which corresponds to a decrease in the configurational entropy.

This apparent paradox is in fact resolved by noting that the decrease in configurational entropy within the shear band pattern is mitigated by the increased plastic dissipation capacity of the shear band. As we have recently shown (Nicot *et al*., 2023; Wang *et al*., 2023), the shear band is an optimal dissipative structure that allows the specimen to resist the shear loading. By the same token, a fluid heated at the bottom should trigger a structuring mechanism through Rayleigh-Bénard convective cells, to undergo the external energy provided beyond a certain level of heating. In fact, this self-organization process is likely to concern any complex systems. This key concept that gathers self-organization, structure, and dissipation through logical links was at the core of Prigogine's developments during the past Century (Prigogine and Lefever, 1968 and 1975; Nicolis and Prigogine, 1977). The configurational granular mechanics proposed herein clearly provides a rational interpretation framework.

As a numerical illustration, Fig. 4 gives the evolution of the normalized configurational entropy, together with the deviatoric stress, along an axial compression under a constant lateral stress of 100 kPa. The same numerical specimen as in Fig. 3 has been used, with a non-zero intergranular friction ($\varphi_g = 35$ deg) between the grains. As expected from the above theoretical framework, the configurational entropy is decreasing (from an initial, arbitrary, zero value), until reaching on average an asymptotic value consistent with the critical state regime.

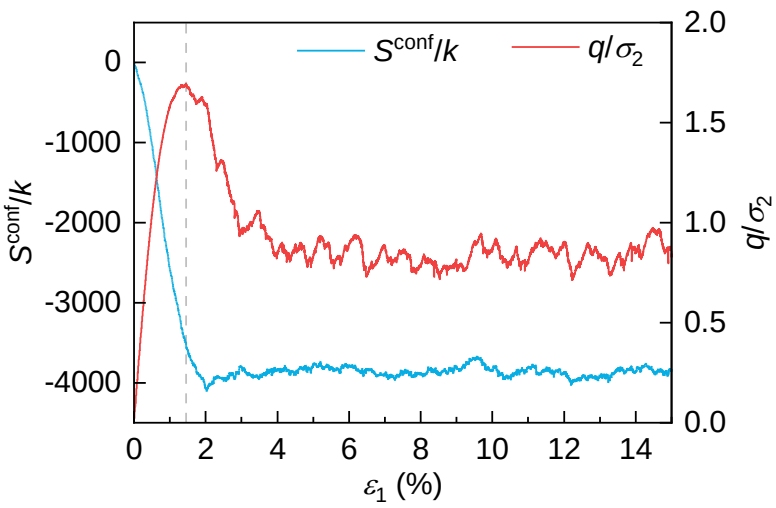

Fig. 4. Simulation of the response of a dense, frictional 2D specimen made up of a polydisperse assembly of 20,000 spherical particles along a biaxial loading under a constant lateral stress of 100 kPa, by using a discrete element method (YADE open-source code, Smilauer *et al*., 2015). The evolution of both the normalized deviatoric stress and the configurational entropy is given in terms of the axial strain.

5.3 Stationary regime and fluctuations

Once a shear band pattern has formed, its topological structure, basically defined through the loop distribution, stays constant on average, which then allows us to describe the critical state regime as a proper stationary regime (Tordesillas, 2007; Zhu *et al*., 2016a; Kuhn, 2016a and 2016b; Deng *et al*., 2021). As a matter of fact, this stationary regime corresponds to the microstate $E^{\mathrm{mic}} = \{(L_3, N_3), (L_4, N_4), \ldots, (L_m, N_m)\}$ staying the same on average with fluctuations in the loop distribution occurring continuously (Zhu *et al*., 2016a and 2016b; Liu *et al*., 2018; Deng *et al*., 2022). In other words, dissipative rearrangements pull the system to a stationary evolution state (Pouragha and Wan, 2021) where configurational changes reach a stationary value dominated by instantaneous, reversible contact gains and loss. More specifically, loop transformations keep on developing, with no effect on the microstate. The configurational reactions $R_{i,j}$ are always active, transforming reversibly the meso-configurations $C(i, 0)$ into the meso-configurations $C(j, i+2-i)$. Locally, the system is configurationally reversible, but these reversible reactions give way to macroscopic irreversibility on the specimen scale.

These configurational reactions can be regarded as local fluctuations (or configurational fluctuations) that develop within the shear band, thereby corresponding to a region undergoing very intense configurational activity. This exhumes the famous paradoxical issue that crossed the past century without finding a clear answer, challenging the fundamental Boltzmann's principle that results from the statistical conception of the second principle of thermodynamics. Any macroscopic system (gas, liquid) brought out of equilibrium experiences a macroscopic irreversibility, in accordance with the second principle, even though the evolution of each microscopic component, basically governed by the second Newton's law, is theoretically reversible. It is worth noting that this paradox was clarified recently through the dissipation theorem (Evans and Searle, 2002). A thorough review discussing this paradox can be found in (Dewar, 2005).

The configurational fluctuations occurring at the critical state correlate with stress fluctuations developing within the granular assembly loaded until the critical state regime takes place. As shown in Fig. 5, where a biaxial loading path is simulated by using a discrete element method, stress fluctuations develop after the stress peak is reached, and become well marked in the

critical state regime. As pointed out in Zhu *et al*. (2016b) and Clerc *et al*. (2021), these stress fluctuations stem from continuous microstructural reorganizations occurring within the assembly. Considering the evolution of two loop categories (loops with 3 grains, and loops with 6 grains), it can be observed in Fig. 6 that the ratios of these two loop categories experience the same fluctuation regime, well correlated with the stress fluctuations displayed in Fig. 5.

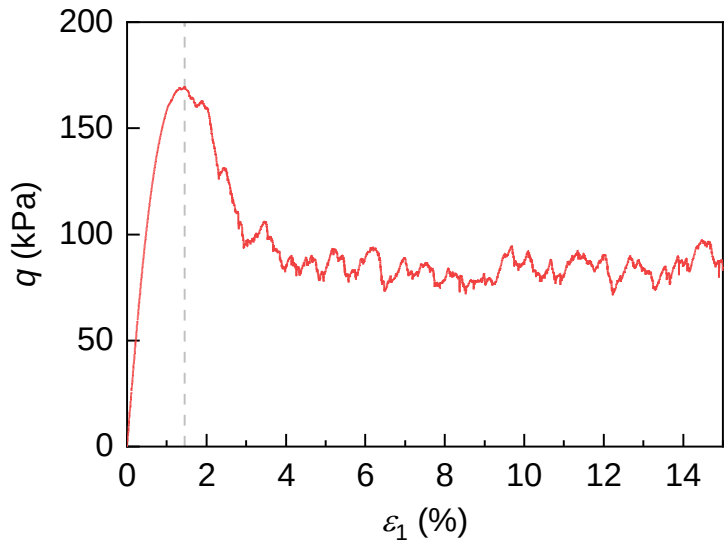

Fig. 5. Simulation of the response of a dense, frictional 2D specimen made up of a polydisperse assembly of 20,000 spherical particles along a biaxial loading under a constant lateral stress σ_2 of 100 kPa, by using a discrete element method (YADE open-source code, Smilauer *et al*., 2015). The evolution of the deviatoric stress $q = \sigma_1 - \sigma_2$ is given in terms of the axial strain.

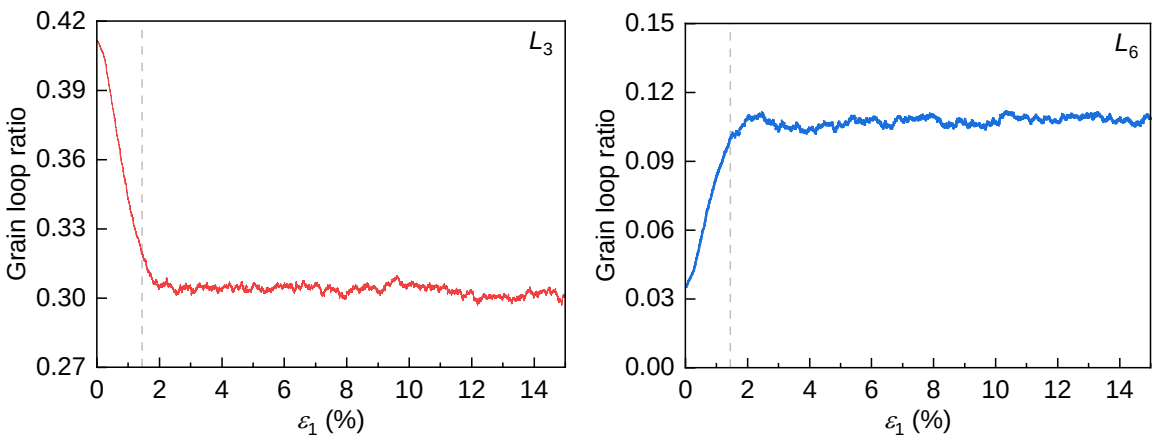

Fig. 6. Evolution of the ratio of two grain loop categories (L_3, left; L_6, right) along a biaxial loading path under constant lateral stress. The fluctuations develop after the deviatoric stress peak is reached, simultaneously with the stress fluctuations (Fig. 3).

The fluctuations in the two loop populations suggest that new loops are continuously created, while older ones disappear through configurational reactions $R_{j,3}$ and $R_{6,k}$ or $R_{l,6}$. Thus, configurational reactions $R_{6,k}$ keep on developing during the critical state regime, even though the loop population distribution is constant on average. Such configurational transformations, inherent in the critical state regime, can be regarded as configurational fluctuations associated with a change in configurational entropy. For example, for a fluctuation $\Delta N_{i,j}$ related to the configurational reactions $R_{i,j}$, the corresponding change in configurational entropy $\Delta S_{i,j}^{conf}$ is given by (Eqs. (14) and (15)):

$$\Delta S_{i,j}^{conf} = -k \ln \frac{(i-1)!}{(j-1)!\,(i+1-j)!} \Delta N_{i,j} = \frac{A_{i,j}}{\theta} \Delta N_{i,j} \tag{36}$$

It is worth noting that $\Delta S_{i,j}^{conf}$ can be positive or negative. This is in accordance with the Boltzmann's statistical approach, as the critical state can be regarded as a stationary state (thermodynamic equilibrium). The local fluctuations $\Delta S_{i,j}^{conf}$ in the configurational entropy are responsible for the global fluctuations that can be observed for the configurational entropy on the specimen scale, as depicted in Figs. 3 and 4.

Finally, by invoking the fluctuation-dissipation theorem (Glansdorff and Prigogine, 1971; Onsager, 1931; Casimir, 1945; Serdyukov, 2022), it should be emphasized that any local increase in entropy will be compensated by a local dissipation involving other configurational transformations elsewhere in the specimen, then ensuring the whole system to be brought back to the thermodynamic equilibrium on the macroscopic scale (Embacher *et al*., 2018; Ledesma-Durán and Santamaría-Holek, 2022; Das *et al*., 2022).

5.4 Closing words

To conclude, it has been demonstrated how granular materials as complex systems are able to adapt and transform under specific loading conditions. The proposed microscopic reinterpretation of granular materials with large numbers of particles as a thermodynamic system within which a configurational entropy and an associated dissipation can be derived represents a plausible framework that certainly needs further investigation. It goes without saying that extending the framework to three-dimensional granular systems should be

regarded as an urgent objective. For such materials, the fabric topology is much more difficult to describe, requiring the concept of 3D grain clusters to be defined in a clear mathematical way. Finally, marrying synergistically complementary subject areas such as statistical physics, fundamental thermodynamics and micromechanics will make it possible to shed a new light on many intriguing mechanisms occurring within complex systems such as granular materials, that have been questioning a broad scientific community since many decades.

ACKNOWLEDGMENTS

We gratefully acknowledge the CNRS International Research Network GeoMech for having offered the opportunity to make this project possible through long-standing collaboration of all the authors (http://gdrmege.univ-lr.fr/).

DECLARATION – DATA AVAILABILITY

The authors declare that they do not have any research data outside the manuscript file.

DECLARATION – ETHICAL APPROVAL

Not applicable

DECLARATION – FUNDING

The authors declare that they do not have received any funding

APPENDIX 1

Positiveness of the configurational affinity $A_{i,j}$

The configurational affinity $A_{i,j}$ is defined by the relation $A_{i,j} = k\,\theta \ln \dfrac{(i-1)!}{(j-1)!\,(i+1-j)!}$. The combinatory term in the logarithm function can be transformed as follows:

$$\frac{(i-1)!}{(j-1)!\,(i+1-j)!} = \left(\frac{i-1}{j-1}\right)\left(\frac{i-2}{j-2}\right)\cdots\left(\frac{i-(j-2)}{2}\right) \tag{A1.1}$$

As $i \geq j+1$, the quotients appearing in Eq. (A1.1) are all strictly greater than 1. Thus:

$$\frac{(i-1)!}{(j-1)!\,(i+1-j)!} > 1 \tag{A1.2}$$

which proves the strict positiveness of all terms $A_{i,j}$, for any couple (i, j) such that $i \in \{4, \ldots, m\}$ and $j < i$

APPENDIX 2

Derivation of Eq. (19)

Starting from Eq. (17), and combining with Eq. (14) gives:

$$\dot{S}^{conf} = -\frac{1}{\theta} \sum_{i=4}^{m} \sum_{j=3}^{\mathrm{int}(i/2)+1} \left(\mu_i - \mu_j - \mu_{i+2-j}\right) \dot{N}_{i,j} \tag{A2.1}$$

which can be rearranged as:

$$\begin{aligned} \dot{S}^{conf} = & -\frac{1}{\theta} \sum_{i=4}^{m-1} \left(\mu_i \left(\sum_{j=3}^{\mathrm{int}(i/2)+1} \dot{N}_{i,j} - \sum_{j=i+1}^{m} \left(1+\delta_{i,j-i+2}\right) \dot{N}_{j,i} \right) \right) \\ & + \frac{1}{\theta} \sum_{i=4}^{m-1} \left(\left(\sum_{j=3}^{\mathrm{int}(i/2)+1} \left(\mu_j + \mu_{i+2-j}\right) \dot{N}_{i,j} - \sum_{j=i+1}^{m} \mu_i \left(1+\delta_{i,j-i+2}\right) \dot{N}_{j,i} \right) \right) \\ & + \frac{1}{\theta} \sum_{j=3}^{\mathrm{int}(m/2)+1} \left(\mu_j + \mu_{m+2-j} - \mu_m\right) \dot{N}_{m,j} \end{aligned} \tag{A2.2}$$

Taking advantage of Eq. (18b), Eq. (A2.2) can be rewritten as:

$$\begin{aligned} \dot{S}^{conf} = & -\frac{1}{\theta} \sum_{i=4}^{m-1} \mu_i \, \dot{N}_i \\ & + \frac{1}{\theta} \sum_{i=4}^{m-1} \left(\left(\sum_{j=3}^{\mathrm{int}(i/2)+1} \left(\mu_j + \mu_{i+2-j}\right) \dot{N}_{i,j} - \sum_{j=i+1}^{m} \mu_i \left(1+\delta_{i,j-i+2}\right) \dot{N}_{j,i} \right) \right) \\ & + \frac{1}{\theta} \sum_{j=3}^{\mathrm{int}(m/2)+1} \left(\mu_j + \mu_{m+2-j} - \mu_m\right) \dot{N}_{m,j} \end{aligned} \tag{A2.3}$$

Using Eqs. (18a) and (18c), we get:

$$\dot{S}^{conf} = -\frac{1}{\theta}\sum_{i=3}^{m}\mu_i\ \dot{N}_i$$
$$+\frac{1}{\theta}\sum_{i=4}^{m-1}\left(\left(\sum_{j=3}^{\mathrm{int}(i/2)+1}\left(\mu_j+\mu_{i+2-j}\right)\dot{N}_{i,j}-\sum_{j=i+1}^{m}\mu_i\left(1+\delta_{i,j-i+2}\right)\dot{N}_{j,i}\right)\right) \tag{A2.4}$$
$$+\frac{1}{\theta}\sum_{j=3}^{\mathrm{int}(m/2)+1}\left(\mu_j+\mu_{m+2-j}\right)\dot{N}_{m,j}-\frac{1}{\theta}\sum_{j=4}^{m}\mu_3\left(1+\delta_{3,j-1}\right)\dot{N}_{j,3}$$

which finally gives:

$$\dot{S}^{conf} = -\frac{1}{\theta}\sum_{i=3}^{m}\mu_i\ \dot{N}_i+\frac{1}{\theta}\dot{\chi} \tag{A2.5}$$

with $\dot{\chi}=\sum_{i=4}^{m}\sum_{j=3}^{\mathrm{int}(i/2)+1}\left(\mu_j+\mu_{i+2-j}\right)\dot{N}_{i,j}-\sum_{i=3}^{m-1}\sum_{j=i+1}^{m}\mu_i\left(1+\delta_{i,j+2-i}\right)\dot{N}_{j,i}$

APPENDIX 3

The objective of this appendix is to demonstrate the nullity of the term:

$$\dot{\chi}=\sum_{i=4}^{m}\sum_{j=3}^{\mathrm{int}(i/2)+1}\left(\mu_j+\mu_{i+2-j}\right)\dot{N}_{i,j}-\sum_{i=3}^{m-1}\sum_{j=i+1}^{m}\mu_i\left(1+\delta_{i,j+2-i}\right)\dot{N}_{j,i}$$

For this purpose, let us introduce the square matrix $\mathbf{M}\in\mathbb{R}_{m,m}$ of general term:

$$\begin{aligned} M_{i,j} &= \left(\mu_j+\mu_{i+2-j}\right)\dot{N}_{i,j} && \text{if } 4\le i\le m \quad\text{and}\quad 3\le j\le \mathrm{int}(i/2)+1 \\ M_{i,j} &= 0 && \text{otherwise} \end{aligned} \tag{A3.1}$$

Thus, the first term $\dot{\chi}_1=\sum_{i=4}^{m}\sum_{j=3}^{\mathrm{int}(i/2)+1}\left(\mu_j+\mu_{i+2-j}\right)\dot{N}_{i,j}$ corresponds to the sum of all the elements of the matrix: $\dot{\chi}_1=\sum_{i=1}^{m}\sum_{j=1}^{m}M_{i,j}$.

Furthermore, $\mathbf{M}$ can be split in two matrixes, $\mathbf{M}=\mathbf{M}^1+\mathbf{M}^2$, with:

$$\begin{aligned} M^1_{i,j} &= \mu_j\ \dot{N}_{i,j} && \text{if } 4\le i\le m \quad\text{and}\quad 3\le j\le \mathrm{int}(i/2)+1 \\ M^1_{i,j} &= 0 && \text{otherwise} \end{aligned} \tag{A3.2}$$

and

$$M^2_{i,j} = \mu_{i+2-j}\ \dot{N}_{i,j} \qquad \text{if } 4 \le i \le m \quad \text{and} \quad 3 \le j \le \text{int}(i/2)+1$$
$$M^2_{i,j} = 0 \qquad \text{otherwise} \tag{A3.3}$$

Both matrices $\mathbf{M}^1$ and $\mathbf{M}^2$ can be transformed by suitable permutation operations into matrices $\mathbf{T}^1$ and $\mathbf{T}^2$, as follows:

$$T^1_{i,j} = M^1_{j,i} \qquad \text{if } 1 \le i \le m \quad \text{and} \quad 1 \le j \le m \tag{A3.4}$$

and

$$T^2_{i,j} = M^1_{i+2-j,i} \qquad \text{if } 1 \le i \le m \quad \text{and} \quad 1 \le j \le m \tag{A3.5}$$

These permutations will induce no change in the term $\dot{\chi}_1 = \sum_{i=1}^{m}\sum_{j=1}^{m} M_{ij}$, so that we have:

$$\dot{\chi}_1 = \sum_{i=1}^{m}\sum_{j=1}^{m} T^1_{i,j} + \sum_{i=1}^{m}\sum_{j=1}^{m} T^2_{i,j} \tag{A3.6}$$

As an illustration, the case where $m = 10$ can be considered:

$$\mathbf{M}^1 = \begin{bmatrix} 0 & 0 & 0 & 0 & 0 & 0 & 0 & 0 & 0 & 0 \\ 0 & 0 & 0 & 0 & 0 & 0 & 0 & 0 & 0 & 0 \\ 0 & 0 & 0 & 0 & 0 & 0 & 0 & 0 & 0 & 0 \\ 0 & 0 & \mu_3\ \dot{N}_{4,3} & 0 & 0 & 0 & 0 & 0 & 0 & 0 \\ 0 & 0 & \mu_3\ \dot{N}_{5,3} & 0 & 0 & 0 & 0 & 0 & 0 & 0 \\ 0 & 0 & \mu_3\ \dot{N}_{6,3} & \mu_4\ \dot{N}_{6,4} & 0 & 0 & 0 & 0 & 0 & 0 \\ 0 & 0 & \mu_3\ \dot{N}_{7,3} & \mu_4\ \dot{N}_{7,4} & 0 & 0 & 0 & 0 & 0 & 0 \\ 0 & 0 & \mu_3\ \dot{N}_{8,3} & \mu_4\ \dot{N}_{8,4} & \mu_5\ \dot{N}_{8,5} & 0 & 0 & 0 & 0 & 0 \\ 0 & 0 & \mu_3\ \dot{N}_{9,3} & \mu_4\ \dot{N}_{9,4} & \mu_5\ \dot{N}_{9,5} & 0 & 0 & 0 & 0 & 0 \\ 0 & 0 & \mu_3\ \dot{N}_{10,3} & \mu_4\ \dot{N}_{10,4} & \mu_5\ \dot{N}_{10,5} & \mu_6\ \dot{N}_{10,6} & 0 & 0 & 0 & 0 \end{bmatrix} \tag{A3.7}$$

$$\mathbf{M}^2 = \begin{bmatrix} 0 & 0 & 0 & 0 & 0 & 0 & 0 & 0 & 0 & 0 \\ 0 & 0 & 0 & 0 & 0 & 0 & 0 & 0 & 0 & 0 \\ 0 & 0 & 0 & 0 & 0 & 0 & 0 & 0 & 0 & 0 \\ 0 & 0 & \mu_3 \dot{N}_{4,3} & 0 & 0 & 0 & 0 & 0 & 0 & 0 \\ 0 & 0 & \mu_4 \dot{N}_{5,3} & 0 & 0 & 0 & 0 & 0 & 0 & 0 \\ 0 & 0 & \mu_5 \dot{N}_{6,3} & \mu_4 \dot{N}_{6,4} & 0 & 0 & 0 & 0 & 0 & 0 \\ 0 & 0 & \mu_6 \dot{N}_{7,3} & \mu_5 \dot{N}_{7,4} & 0 & 0 & 0 & 0 & 0 & 0 \\ 0 & 0 & \mu_7 \dot{N}_{8,3} & \mu_6 \dot{N}_{8,4} & \mu_5 \dot{N}_{8,5} & 0 & 0 & 0 & 0 & 0 \\ 0 & 0 & \mu_8 \dot{N}_{9,3} & \mu_7 \dot{N}_{9,4} & \mu_6 \dot{N}_{9,5} & 0 & 0 & 0 & 0 & 0 \\ 0 & 0 & \mu_9 \dot{N}_{10,3} & \mu_8 \dot{N}_{10,4} & \mu_7 \dot{N}_{10,5} & \mu_6 \dot{N}_{10,6} & 0 & 0 & 0 & 0 \end{bmatrix} \tag{A3.8}$$

And after transformation, we get:

$$\mathbf{T}^1 = \begin{bmatrix} 0 & 0 & 0 & 0 & 0 & 0 & 0 & 0 & 0 & 0 \\ 0 & 0 & 0 & 0 & 0 & 0 & 0 & 0 & 0 & 0 \\ 0 & 0 & 0 & \mu_3 \dot{N}_{4,3} & \mu_3 \dot{N}_{5,3} & \mu_3 \dot{N}_{6,3} & \mu_3 \dot{N}_{7,3} & \mu_3 \dot{N}_{8,3} & \mu_3 \dot{N}_{9,3} & \mu_3 \dot{N}_{10,3} \\ 0 & 0 & 0 & 0 & 0 & \mu_4 \dot{N}_{6,4} & \mu_4 \dot{N}_{7,4} & \mu_4 \dot{N}_{8,4} & \mu_4 \dot{N}_{9,4} & \mu_4 \dot{N}_{10,4} \\ 0 & 0 & 0 & 0 & 0 & 0 & 0 & \mu_5 \dot{N}_{8,5} & \mu_5 \dot{N}_{9,5} & \mu_5 \dot{N}_{10,5} \\ 0 & 0 & 0 & 0 & 0 & 0 & 0 & 0 & 0 & \mu_6 \dot{N}_{10,6} \\ 0 & 0 & 0 & 0 & 0 & 0 & 0 & 0 & 0 & 0 \\ 0 & 0 & 0 & 0 & 0 & 0 & 0 & 0 & 0 & 0 \\ 0 & 0 & 0 & 0 & 0 & 0 & 0 & 0 & 0 & 0 \\ 0 & 0 & 0 & 0 & 0 & 0 & 0 & 0 & 0 & 0 \end{bmatrix} \tag{A3.9}$$

and

$$\mathbf{T}^2 = \begin{bmatrix} 0 & 0 & 0 & 0 & 0 & 0 & 0 & 0 & 0 & 0 \\ 0 & 0 & 0 & 0 & 0 & 0 & 0 & 0 & 0 & 0 \\ 0 & 0 & 0 & \mu_3 \dot{N}_{4,3} & 0 & 0 & 0 & 0 & 0 & 0 \\ 0 & 0 & 0 & 0 & \mu_4 \dot{N}_{5,3} & \mu_4 \dot{N}_{6,4} & 0 & 0 & 0 & 0 \\ 0 & 0 & 0 & 0 & 0 & \mu_5 \dot{N}_{6,3} & \mu_5 \dot{N}_{7,4} & \mu_5 \dot{N}_{8,5} & 0 & 0 \\ 0 & 0 & 0 & 0 & 0 & 0 & \mu_6 \dot{N}_{7,3} & \mu_6 \dot{N}_{8,4} & \mu_6 \dot{N}_{9,5} & \mu_6 \dot{N}_{10,6} \\ 0 & 0 & 0 & 0 & 0 & 0 & 0 & \mu_7 \dot{N}_{8,3} & \mu_7 \dot{N}_{9,4} & \mu_7 \dot{N}_{10,5} \\ 0 & 0 & 0 & 0 & 0 & 0 & 0 & 0 & \mu_8 \dot{N}_{9,3} & \mu_8 \dot{N}_{10,4} \\ 0 & 0 & 0 & 0 & 0 & 0 & 0 & 0 & 0 & \mu_9 \dot{N}_{10,3} \\ 0 & 0 & 0 & 0 & 0 & 0 & 0 & 0 & 0 & 0 \end{bmatrix} \tag{A3.10}$$

It is worth noting that the matrix $\mathbf{T} = \mathbf{T}^1 + \mathbf{T}^2$ takes the convenient form:

$$\mathbf{T} = \begin{bmatrix} 0 & 0 & 0 & 0 & 0 & 0 & 0 & 0 & 0 & 0 \\ 0 & 0 & 0 & 0 & 0 & 0 & 0 & 0 & 0 & 0 \\ 0 & 0 & 0 & 2\mu_3\,\dot{N}_{4,3} & \mu_3\,\dot{N}_{5,3} & \mu_3\,\dot{N}_{6,3} & \mu_3\,\dot{N}_{7,3} & \mu_3\,\dot{N}_{8,3} & \mu_3\,\dot{N}_{9,3} & \mu_3\,\dot{N}_{10,3} \\ 0 & 0 & 0 & 0 & \mu_4\,\dot{N}_{5,3} & 2\mu_4\,\dot{N}_{6,4} & \mu_4\,\dot{N}_{7,4} & \mu_4\,\dot{N}_{8,4} & \mu_4\,\dot{N}_{9,4} & \mu_4\,\dot{N}_{10,4} \\ 0 & 0 & 0 & 0 & 0 & \mu_5\,\dot{N}_{6,3} & \mu_5\,\dot{N}_{7,4} & 2\mu_5\,\dot{N}_{8,5} & \mu_5\,\dot{N}_{9,5} & \mu_5\,\dot{N}_{10,5} \\ 0 & 0 & 0 & 0 & 0 & 0 & \mu_6\,\dot{N}_{7,3} & \mu_6\,\dot{N}_{8,4} & \mu_6\,\dot{N}_{9,5} & 2\mu_6\,\dot{N}_{10,6} \\ 0 & 0 & 0 & 0 & 0 & 0 & 0 & \mu_7\,\dot{N}_{8,3} & \mu_7\,\dot{N}_{9,4} & \mu_7\,\dot{N}_{10,5} \\ 0 & 0 & 0 & 0 & 0 & 0 & 0 & 0 & \mu_8\,\dot{N}_{9,3} & \mu_8\,\dot{N}_{10,4} \\ 0 & 0 & 0 & 0 & 0 & 0 & 0 & 0 & 0 & \mu_9\,\dot{N}_{10,3} \\ 0 & 0 & 0 & 0 & 0 & 0 & 0 & 0 & 0 & 0 \end{bmatrix} \tag{A3.11}$$

Generalizing to any order m, it follows that the general term of the two matrices $\mathbf{T}^1$ and $\mathbf{T}^2$ reads:

$$\begin{aligned} &T^1_{i,j} = \mu_i\,\dot{N}_{j,i} && \text{if } 3 \le i \le \text{int}(m/2)+1 \quad \text{and} \quad 2(i\text{-}1) \le j \le m \\ &T^1_{i,j} = 0 && \text{otherwise} \end{aligned} \tag{A3.12}$$

Likewise:

$$\begin{aligned} &T^2_{i,j} = \mu_i\,\dot{N}_{j,j+2-i} && \text{if } 3 \le i \le \text{int}(m/2)+1 \quad \text{and} \quad i+1 \le j \le 2(i-1) \\ &T^2_{i,j} = \mu_i\,\dot{N}_{j,j+2-i} && \text{if } \text{int}(m/2)+2 \le i \le m-1 \quad \text{and} \quad i+1 \le j \le m \\ &T^2_{i,j} = 0 && \text{otherwise} \end{aligned} \tag{A3.13}$$

Thus, the particular form of the matrices $\mathbf{T}^1$ and $\mathbf{T}^2$ allows us to write:

$$\sum_{i=1}^{m}\sum_{j=1}^{m} T^1_{i,j} = \sum_{i=3}^{\text{int}(m/2)+1}\ \sum_{j=2(i-1)}^{m} \mu_i\,\dot{N}_{j,i} \tag{A3.14}$$

$$\sum_{i=1}^{m}\sum_{j=1}^{m} T^2_{i,j} = \sum_{i=3}^{\text{int}(m/2)+1}\ \sum_{j=i+1}^{2(i-1)} \mu_i\,\dot{N}_{j,j+2-i} + \sum_{i=\text{nt}(m/2)+2}^{m-1}\ \sum_{j=i+1}^{m} \mu_i\,\dot{N}_{j,j+2-i} \tag{A3.15}$$

Recalling now that $\dot{N}_{j,j+2-i} = \dot{N}_{j,i}$, Eqs. (A3.14) and (A3.15) yield:

$$\dot{\chi}_1 = \sum_{i=3}^{\text{int}(m/2)+1}\ \sum_{j=2(i-1)}^{m} \mu_i\,\dot{N}_{j,i} + \sum_{i=3}^{\text{int}(m/2)+1}\ \sum_{j=i+1}^{2(i-1)} \mu_i\,\dot{N}_{j,i} + \sum_{i=\text{nt}(m/2)+2}^{m-1}\ \sum_{j=i+1}^{m} \mu_i\,\dot{N}_{j,i} \tag{A3.16}$$

The summation $\sum_{i=3}^{\mathrm{int}(m/2)+1} \sum_{j=2(i-1)}^{m} \mu_i \dot{N}_{j,i} + \sum_{i=3}^{\mathrm{int}(m/2)+1} \sum_{j=i+1}^{2(i-1)} \mu_i \dot{N}_{j,i}$ can be merged in one single term, after noting that the index $j = 2(i-1)$ is counted twice. As this corresponds to $i = j + 2 - i$, it is convenient to introduce the Kronecker symbol $\delta_{i,j+2-i}$, so that:

$$\sum_{i=3}^{\mathrm{int}(m/2)+1} \sum_{j=2(i-1)}^{m} \mu_i \dot{N}_{j,i} + \sum_{i=3}^{\mathrm{int}(m/2)+1} \sum_{j=i+1}^{2(i-1)} \mu_i \dot{N}_{j,i} = \sum_{i=3}^{\mathrm{int}(m/2)+1} \sum_{j=i+1}^{m} \mu_i \left(1+\delta_{i,j+2-i}\right) \dot{N}_{j,i} \tag{A3.17}$$

Furthermore, as $j \le m$ $j = 2(i-1)$ requires that $i \le \mathrm{int}(m/2)+1$. Thus, the third term $\sum_{i=\mathrm{nt}(m/2)+2}^{m-1} \sum_{j=i+1}^{m} \mu_i \dot{N}_{j,i}$ can also be expressed as:

$$\sum_{i=\mathrm{nt}(m/2)+2}^{m-1} \sum_{j=i+1}^{m} \mu_i \dot{N}_{j,i} = \sum_{i=\mathrm{nt}(m/2)+2}^{m-1} \sum_{j=i+1}^{m} \mu_i \left(1+\delta_{i,j+2-i}\right) \dot{N}_{j,i} \tag{A3.18}$$

Finally, combining Eq. (A3.16) with (A3.17) and (A3.18) yields:

$$\dot{\chi}_1 = \sum_{i=3}^{m-1} \sum_{j=i+1}^{m} \mu_i \left(1+\delta_{i,j+2-i}\right) \dot{N}_{j,i} \tag{A3.19}$$

which proves that $\dot{\chi} = 0$

REFERENCES

Adam, G., and Gibbs, J.H. (1965): On the temperature dependence of cooperative relaxation properties in glass-forming liquids. J. Chem. Phys., Vol. 43, 139.

Baule, A., Morone, F., Herrmann, H.J., and Makse, H.A. (2018): Edwards statistical mechanics for jammed granular matter. Rev. Mod. Phys., Vol. 90, 015006.

Been, K., Jefferies, M., and Hachey, J. (1991): The critical state of sands. Geotechnique, Vol. 41, 365.

Bénard, H. (1901): Les tourbillons cellulaires dans une nappe liquide transportant de la chaleur par convection en régime permanent. Annales de chimie et de physique, Vol. 7(23), pp. 62-144.

Benfenati, F., and Beretta, G.P. (2018): Ergodicity, maximum entropy production, and steepest entropy ascent in the proofs of Onsager's reciprocal relations. Journal of Non-

Equilibrium Thermodynamics, Vol. 43(2), pp. 101-110. https://doi.org/10.1515/jnet-2017-0054.

Bi, D., Henkes, S., Daniels, K.E., and Chakraborty, B. (2015): The statistical physics of athermal materials. Annu. Rev. Condensed Matter Phys., Vol. 6, pp. 63–83.

Blumenfeld, R., and Edwards, S. (2014): Granular statistical mechanics – a personal perspective. Eur. Phys. J. Spec. Top., Vol. 223, pp. 2189–2204.

Blumenfeld, R., and Edwards, S.F. (2003): Granular entropy: explicit calculations for planar assemblies. Phys Rev Lett, Vol. 90, 114303.

Boltzmann, L. (1877): Uber die Beziehung eines allgemeine mechanischen Satzes zum zweiten Hauptsatze der Warmetheorie. Sitzungsberichte der Akademie der Wissenschaften, Wien, II, 75, 67-73 [English translation in: S.G. Brush, Kinetic theory, Vol. 2, Irreversible processes, pp. 188-193, Pergamon Press, Oxford (1966)].

Casimir, H. (1945): On Onsager's Principle of Microscopic Reversibility. Reviews of Modern Physics, Vol. 17, p. 343.

Clerc, A., Wautier, A., Bonelli, S., and Nicot, F. (2021): Meso-scale signatures of inertial transitions in granular materials. Granular Matter, Vol. 23 (2), pp. 24-28.

Cundall, P.A, and Strack, O.D.L. (1979): A discrete numerical model for granular assemblies. Geotechnique, Vol. 29(1), pp. 47-65.

Das, S., Ghosh, S., and Gupta, S. (2022): State-dependent driving: a route to non-equilibrium stationary states. Proc. R. Soc. A., Vol. 478, 20210885.

Deng, N., Wautier, A., Thiery, Y., Yin, Z.Y., Hicher, P.Y., and Nicot, F. (2021): On the attraction power of critical state in granular materials. J. Mech. and Physics of Solids, Vol. 149, 104300.

Deng, N., Wautier, A., Tordesillas, A., Thiery, Y., Yin, Z.Y., Hicher, P.Y., and Nicot, F. (2022): Lifespan dynamics of cluster conformations in stationary regimes in granular materials. Physical Review/E, in press.

De Gennes, P.G., Brochard-Wyart, F., and Quéré, D. (2002) : Gouttes, bulles, perles et ondes. Belin Ed.

Desrues, J., and Andò, E. (2015): Strain localisation in granular media. Comptes Rendus. Physique, Académie des sciences (Paris), Vol. 16 (1), pp.26-36.

Dewar, R. C. (2005). Maximum entropy production and the fluctuation theorem. Journal of Physics A: Mathematical and General, 38(21): L371-L381.

Doig, A.J., and Sternberg, M.J.E. (1995): Side-chain conformational entropy in protein folding. Protein Science, Vol. 4, pp. 2247-2251.

Duran, J. (2000): Sands, Powders, and Grains: An introduction to the physics of granular material. Springer-Verlag, New York.

Edwards, S.F., and Oakeshott, R.B.S. (1989): Theory of powders. Physica A: Statistical Mechanics and its Applications, Vol. 157(3), pp. 1080–1090.

Einstein, A. (1905): Uber die von der molekularkinetischen theorie der wärme geforderte bewegung von in ruhenden flüssigkeiten suspendierten teilchen. Annalen der Physik, Vol. 17, pp. 549-560.

Embacher, P., Dirr, N., Zimmer, J., and Reina, C. (2018): Computing diffusivities from particle models out of equilibrium. Proc. R. Soc. A., Vol. 474, 20170694.

Evans, D., and Searle, D. (2002): The fluctuation theorem. Advances in Physics, 51(7): 1529-1585.

Gibbs, J.H., and DiMarzio, E.A. (1958): Nature of the glass transition and the glassy state J. Chem. Phys., Vol. 28, 373.

Gibbs, J.W. (1902): Elementary Principles in Statistical Mechanic. New York, Charles Scribner's Sons Publ.

Glansdorff, P., and Prigogine, I. (1954): Sur les propriétés différentielles de la production d'entropie. Physica, Vol. 20(7-12), pp. 773–780.

Glansdorff, P., and Prigogine, I. (1963): Generalised entropy production and hydrodynamic stability. Physics Letters, Vol. 7(4), pp. 243–244.

Glansdorff, P., and Prigogine, I. (1964): On a general evolution criterion in macroscopic physics. Physica, Vol. 30(2), pp. 351–374.

Glansdorff, P., and Prigogine, I. (1971): Thermodynamic theory of structure, stability and fluctuations. Wiley-Intersçience, N.Y.

Goldhirsch, I. (2008): Introduction to granular temperature. Powder Technology, Vol. 182, Issue 2, pp. 130-136.

Hudson, J.L., and Mankin, J.C. (1981). Chaos in the Belousov–Zhabotinskii reaction. J. Chem. Phys., Vol. 74 (11), pp. 6171–6177.

Jaeger, H.M., Nagel, S.R., and Behringer, R.P. (1996): Granular solids, liquid, and gases. Rev. Mod. Phys., Vol. 68:1259.

Janečka, A., and Pavelka, M. (2018): Gradient dynamics and entropy production maximization. Journal of Non-Equilibrium Thermodynamics, Vol. 43(1), pp. 1-19. https://doi.org/10.1515/jnet-2017-0005.

Jaynes, E.T. (1957): Information Theory and Statistical Mechanics. Phys. Rev., Vol. 106, 620.

Jaynes, E.T. (1983): Papers on Probability, Statistics and Statistical Physics. Edited by R. D. Rosenkrantz, D. Reidel Publishing Co., Dordrecht, Holland.

Kadanoff L. P. (1999): Built upon sand: Theoretical ideas inspired by granular flows. Rev. Mod. Phys., Vol. 71:43.

Kuhn, M. R. (2016a): The critical state of granular media: Convergence, stationarity and disorder. Géotechnique, Vol. 66, 902.

Kuhn, M. R. (2016b): Maximum disorder model for dense steady-state flow of granular materials. Mech. Mater., Vol. 93, 63.

Ledesma-Durán, A., and Santamaría-Holek, I. (2022): Energy and entropy in open and irreversible chemical reaction–diffusion systems with asymptotic stability. Journal of Non-Equilibrium Thermodynamics, Vol. 47(3), pp. 311-328. https://doi.org/10.1515/jnet-2022-0001.

Liu, A., and Nagel, S. (1998): Jamming is not just cool any more. Nature, Vol. 396, pp. 21–22.

Liu, J., Nicot, F., and Zhou, W. (2018): Sustainability of internal structures during shear band forming in 2D granular materials. Powder Technology, Vol. 338, pp. 458–470.

Liu, J., Wautier, A., Bonelli, S., Nicot, F., and Darve, F. (2020): Macroscopic softening in granular materials from a mesoscale perspective. Int. J. Solids Structures, 93-194, pp. 222-238. DOI 10.1016/j.ijsolstr.2020.02.022.

Lucarini, V., Pavliotis, G.A., and Zagli N. (2020): Response theory and phase transitions for the thermodynamic limit of interacting identical systems. Proceedings of the Royal Society A, Vol. 476(2244), 20200688.

Maxwell, J. C. (1860): Illustrations of the dynamical theory of gases. Part I. On the motions and collisions of perfectly elastic spheres. The London, Edinburgh, and Dublin Philosophical Magazine and Journal of Science, Vol. 19, pp. 19-32.

Nicolis, G., and Prigogine, I. (1977), Self-Organization in Nonequilibrium Systems: From Dissipative Structures to Order through Fluctuations. New York, John Wiley & Sons.

Nicot, F., and Darve, F. (2007): Basic features of plastic strains: from micro-mechanics to incrementally nonlinear models. Int. Journal of Plasticity, Vol. 23, pp. 1555-1588.

Nicot, F., Wang, X., Wautier, A., Wan, R., and Darve, F. (2023): Shear banding as a dissipative structure from a thermodynamic viewpoint. Journal of the Mechanics and Physics of Solids, Vol. 179, 105394.

Onsager, L. (1931): Reciprocal Relations in Irreversible Processes (I). Physical Review, Vol. 37, p. 405.

Parisi, G. (2012): Disordered systems and neural networks. arXiv:1201.5813 [cond-mat.dis-nn], https://doi.org/10.48550/arXiv.1201.5813.

Parisi, G., Procaccia, I., Rainone, C., Singh, M. (2017): Shear bands as manifestation of a criticality in yielding amorphous solids. Proc. Natl. Acad. Sci. U. S. A., Vol. 114, pp. 5577–5582. https://doi.org/10.1073/pnas.1700075114.

Peters, J. F., Muthuswamy, M., Wibowo, J., and Tordesillas, A. (2005): Characterization of force chains in granular material. Physical review E, Vol. 72 (4), 041307.

Porporato, A., Hooshyar, M., Bragg A.D., and Katul, G. (2020): Fluctuation theorem and extended thermodynamics of turbulence. Proc. R. Soc. A., Vol. 476, 20200468.

Pouragha, M., and Wan, R. (2021): μ-GM: A purely micromechanical constitutive model for granular materials, Mechanics of Materials, Vol. 126, pp. 57-74,

Preisler, Z., and Dijkstra, M. (2016): Configurational entropy and effective temperature in systems of active Brownian particles. Soft Matter, Vol. 12, pp. 6043-6048.

Prigogine, I., and Lefever, R. (1968): Symmetry Breaking Instabilites in Dissipative Systems. The Journal of Chemical Physics, vol. 48, no 4, pp. 1695–1700.

Prigogine, I., and Lefever, R. (1975): Stability and Self-Organization in Open Systems. Advances in Chemical Physics, Vol. 29, pp. 1–28.

Pucilowski S., and Tordesillas, A. (2020): Rattler wedging and force chain buckling: Metastable attractor dynamics of local grain rearrangements underlie globally bistable shear banding regime. Granular Matter, Vol. 22, 18.

Pucilowski, S., and Tordesillas, A. (2020): Rattler wedging and force chain buckling: Metastable attractor dynamics of local grain rearrangements underlie globally bistable shear banding regime. Granular Matter, Vol. 22, 18.

Radjai, F., Wolf, D.E., Jean, M., Moreau, J.-J. (1998): Bimodal character of stress transmission in granular packings. Physical review letters, Vol. 80 (1), 61.

Rayleigh, J. W. (1916): On convection currents in a horizontal layer of fluid, when the higher temperature is on the underside. The London, Edinburgh, and Dublin Philosophical Magazine and Journal of Science, Sixth series, Vol.32(192), pp. 529-546.

Roscoe, K. H., Schofield, A., and Wroth, A. P. (1958): On the yielding of soils. Geotechnique, Vol. 8, 22.

Serdyukov, S.I. (2022): The Onsager–Machlup theory of fluctuations and time-dependent generalized normal distribution. Journal of Non-Equilibrium Thermodynamics, Vol. 48, no. 3, pp. 243-254. https://doi.org/10.1515/jnet-2022-0071.

Serero, C., Goldenberg, S., Noskowicz, H., and Goldhirsch, I. (2008): The classical granular temperature and slightly beyond. Powder Technology, Vol. 182, Issue 2, pp. 257-271.

Shannon, C.E. (1948): A mathematical theory of communication. Bell System Technical Journal, Vol. 27, pp. 379-423.

Silbert, L. E. (2005): Temporally heterogeneous dynamics in granular flows. Physical Review Letters, Vol. 94(9), 098002.

Smilauer, V., et al. (2015): Yade Documentation 2nd ed (The Yade Project, 2015) http://yade-dem.org/doc/.

Sun, X., Kob, W., Blumenfeld, R., Tong, H, Wang, Y., and Zhang J. (2020): Friction-controlled entropy-stability competition in granular systems. Phys. Rev. Lett., Vol. 125, 268005.

Tordesillas, A. (2007): Force chain buckling, unjamming transitions and shear banding in dense granular assemblies. Phil. Mag. Vol. 87(32), pp. 4987-5016.

Tordesillas, A., Walker, D. M., Froyland, G., Zhang, J., and Behringer, R.P. (2012): Transition dynamics and magic-number-like behavior of frictional granular clusters. Phys. Rev. E, Vol. 86, 011306.

Tordesillas, A., Walker, D.M., Froyland, G., Zhang, J., and Behringer, R.P. (2012): Transition dynamics and magic-number-like behavior of frictional granular clusters, Phys. Rev. E, Vol. 86, 011306.

Veveakis, E., and Regenauer-Lieb, K. (2015): Review of extremum postulates. Current Opinion in Chemical Engineering, 7(C), pp. 40-46.

Walker, D. M., Tordesillas, A., Brodu, N., Dijksman, J. A., Behringer, R. P., and Froyland, G. (2015): Self-assembly in a near frictionless granular material: Conformational structures and transitions in uniaxial cyclic compression of hydrogel spheres. Soft Matter, Vol. 11, 2157.

Walker, D.M., Tordesillas, A., Brodu, N., Dijksman, J.A., Behringer, R.P., and Froyland, G. (2015): Self-assembly in a near-frictionless granular material: Conformational structures and transitions in uniaxial cyclic compression of hydrogel spheres. Soft matter, Vol. 11, 2157.

Wan, R., Nicot, F., and Darve, F. (2017): Failure in geomaterials, a contemporary treatise. Ed. ISTE-Wiley, 222 pages.

Wang, X., Liu, Y, and Nicot, F. (2023): Energy processes and phase transition in granular assemblies. Int. J. of Solids and Structures, under review.

Wanjura, C.C., Gago, P., Matsushima, T., and Blumenfeld, R. (2020): Structural evolution of granular systems: theory. Granular Matter, Vol. 22(91), https://doi.org/10.1007/s10035-020-01056-4

Ziegler, H. (1983): An Introduction to Thermomechanics. Amsterdam, North Holland.

Zhu, H., Nguyen, Hien N.G., Nicot, F., and Darve, F. (2016a): On a common critical state in localized and diffuse failure modes. J. Mechanics and Physics of Solids, Vol. 95, pp. 112–131. doi: 10.1016/j.jmps.2016.05.026.

Zhu, H., Nicot, F., and Darve, F. (2016b): Meso-structure organization in two-dimensional granular materials along biaxial loading path. Int. J. Solids and Structures, Vol. 96, pp. 25-37.